

# Towards Assessing Cycleway Pavement Surface Roughness Using an Action Camera with IMU and GPS

Muhammad Hassam Baig<sup>1,2</sup><sup>a</sup>, Jeziel Antonio Ayala Garcia<sup>1</sup><sup>b</sup>, Waqar Shahid Qureshi<sup>1</sup><sup>c</sup>  
and Ihsan Ullah<sup>1,2</sup><sup>d</sup>

<sup>1</sup>*School of Computer Science, University of Galway, Galway, Ireland*

<sup>2</sup>*Data Science Institute, University of Galway, Galway, Ireland*

**Keywords:** Action Camera, Cycleways, Corrected Roughness Index, Greenways, International Roughness Index, Pavement Roughness, Quarter Car Model, Rolling Variance, Stability.

**Abstract:** This paper introduces an autonomous and cost-effective method for assessing cycleway pavement roughness, using an action camera equipped with high-resolution sensors including an Inertial Measurement Unit (IMU) and a Global Positioning System (GPS). The methodology utilizes simplified quarter car model for bicycles, without manual intervention, to calculate International Roughness Index (IRI) for cycleway surface quality evaluation. It utilizes our novel approach to determine stable section from which average acceleration orientation vector is computed. For analysis we propose a corrected-roughness index (CRI), which is a quantized version of IRI. Experiments conducted on asphalt cycleways in Ireland revealed strong correlations between vehicle vibration and surface roughness. Results further demonstrate the consistency of the proposed model across different bikes through comparative analysis. Observations indicate bias in vibration data, influenced by different tire sizes and the mechanical features of the bicycles.

## 1 INTRODUCTION

Pavement surface roughness is a key indicator of pavement quality, directly affecting user comfort. As greenways wear down over time, irregularities negatively impact cycle performance, increase maintenance costs and compromise safety. Measuring and analysing pavement roughness is crucial for maintaining cycleways, guiding infrastructure investments, and ensuring user satisfaction.

Pavement roughness has been previously assessed through various methods such as Present serviceability index, IRI, Mean ride index etc., but recent advancements in technology have led to more cost-effective approaches (Hettiarachchi, Yuan, Amirkhani and Xiao, 2023).

Process of measuring pavement roughness changed a lot in the last few decades, growing rapidly with the help of advanced tools and technologies, due

to the demand of accurate, time-effective and cost-effective methods to calculate road roughness. Table 1 enlists some of the instruments, sensors, measurement methods along with their pavement roughness measurement year.

Initially, pavement roughness was measured with mechanical systems such as profilograph, that measure vertical deviations on a road's surface by means of wheels and beams. This was later replaced by non-contact profilers which measure vehicle responses to roughness that yield indirect estimates of the profile (Woodstrom, 1990).

One of the most significant changes occurred in the 1986 when Sayers, Gillespie and Queiroz (1986) from Federal Highway Administration, established the use of the IRI for roughness calculation as a standard. The authors utilized quarter car model, a simplified representation of a car's suspension system, to compute IRI.

<sup>a</sup>  <https://orcid.org/0009-0003-3153-9527>

<sup>b</sup>  <https://orcid.org/0009-0006-7829-9948>

<sup>c</sup>  <https://orcid.org/0000-0003-0176-8145>

<sup>d</sup>  <https://orcid.org/0000-0002-7964-5199>

Around 1990s, inertial profilers were utilizing accelerometers and lasers for increased accuracy and efficiency, before the implementation of laser-only devices. Advances continued into the following decades with the use of 3D imaging systems mounted with scanning lasers and reflectors to produce detailed digital profiles of pavement surfaces for evaluations of road conditions, such as roughness, rutting, and cracking (Fares and Zayed, 2023).

Since the 2010s and beyond the research has been moved towards automated low-cost systems. The studies show common use of available technology such as smartphones and IoT systems for the measurement of pavement roughness (Kumar, Tallam and Kumar, 2022; Zhang and Wenjiang, 2022; Yu, Fang and Wix, 2022; Alatoon and Obaidat, 2022). The accuracy and reliability of such measurements have been greatly improved by the integration of advanced analytical techniques along with machine learning models. The validation of these methodologies against professional instruments demonstrates their potential for increasing accessibility to a wide user group.

Today, devices equipped with sensors such as lidar, laser, IMU and GPS offer efficient solutions to measure road conditions. These devices capture precise data regarding the surface deviations of roads and can also be used for cycleways, which are often overlooked in traditional assessments.

Zang, Shen, Huang, Wan and Shi, (2018) developed a new methodology for computing IRI using simplified quarter car model for bicycles. They collected road surface data by mounting smartphone over the handlebar of the bicycle and captured sensor data. Compared the results with laser pavement scanner, a professional instrument, and reported significant associations with it.

However, their methodology involves manual interpretation of average acceleration vector. For this purpose, authors had to ask the bicycle riders to maintain the speed and posture as stable as possible for initial 5 seconds.

Similarly, Rizelioğlu and Yazıcı, (2024) used a mountain bike to obtain road roughness measurement

using the quarter car model, by sensors, accelerometer (MPU-6050) and GPS (NEO-6), then compared the measurements with reference, laser profilometer device results. The results were close to reference IRI values. To develop the method considerably, they suggest further studies into alternate wheel characteristics and types of roads. It adds weight to the idea that sensor-equipped bicycles can be practically useful for evaluating road roughness.

To generate real time IRI maps, integration of accelerometers and GPS sensors with microcontrollers was also under consideration. The validity of this system is confirmed by correlation with smartphone data (Hafizh, Abdullah, Ateeq, Majeed, Isaac, and Hu, 2023). It suggested that adding variety of roads and environment condition would help evaluate the accuracy of measurements, emphasizing the flexibility of IoT systems.

This study presents a forward-looking approach for autonomously monitoring cycle path surface roughness using readily available components. With cycling infrastructure expanding globally and a growing emphasis on sustainability and active transportation, the need for efficient and accurate surface monitoring technologies becomes increasingly crucial.

Our research builds upon the framework established by Zang et al. (2018) for calculating pavement roughness using bicycles. We further develop their approach to autonomously calculate IRI to assess surface quality of cycleways without manual intervention. The system's automation eliminates human variability in posture and speed, providing consistent and accurate measurements. This approach enables large-scale deployment and continuous monitoring without manual intervention, making it cost-effective and user-friendly.

The core of our methodology is a refined technique for determining the average acceleration orientation vector by finding stable section, autonomously. To further enhance the analytical robustness of our assessments, we introduce the CRI, a quantized version of the traditional IRI. This new

Table 1: Provides list of the instruments, sensors, measurement methods with year of pavement roughness measurement.

| Instrument                   | Sensor   | Method                        | Year |
|------------------------------|--|-------------------------------|------|
| Mays Meter                   | Accelerometer  | Bump Integrator               | 1962 |
| Profilograph                 | Inclinometer, Accelerometer                                  | Profile Index                 | 1966 |
| Contact Profiling Device     | Inertial Measurement units                                   | Pavement Condition Index      | 1973 |
| Dipstick                     | Laser, Inclinometer  | Profilograph Index            | 1980 |
| South Dakota Road Profiler   | Laser, Inertial Measurement Units, Global positioning system | International roughness Index | 1986 |
| Non-contact profiling device | Laser, Optical   | Half Car roughness Index      | 1986 |

index provides generic assessment of surface roughness specifically tailored to cycleways. In the subsequent sections, we discuss the mathematical model of the simplified quarter car model adapted for bicycles, the rationale behind finding stable section, detailed descriptions of our proposed methodology, results and conclusion.

## 2 MATHEMATICAL BACKGROUND

First, we will present the mathematical model as described for roughness calculation by Zang, Shen, Huang, Wan and Shi, (2018). They developed the quarter car model for bicycles to calculate IRI, providing all the necessary mathematical proofs. The researchers explain that the pavement's signature is determined from the longitudinal profile of the path, with the profile's vertical displacement being quantified in equation 1.

$$D_i = |h_i - h_{i-1}| \text{ for all } i \geq 1 \quad (1)$$

Where  $D$  is vertical displacement,  $i$  is the sampling time,  $h$  is height. Vertical displacement data captured by action camera is prone to huge errors thus we cannot rely on it. Thus, we calculate vertical displacement using accelerometer by utilizing the formulas from physics as shown in equation 2.

$$\begin{aligned} V_v &= \frac{dD}{dt} \\ \alpha_v &= \frac{d^2D}{dt^2} \end{aligned} \quad (2)$$

Where  $V_v$  is vertical speed and  $\alpha_v$  is vertical acceleration. This leads to vertical displacement, equation 3.

$$\sum D = \iint_{tstart}^{tstop} |\alpha_v|(dt)^2 \quad (3)$$

Since orientation of bicycle and action camera are variable. The vertical acceleration ( $\alpha_v$ ) can appear in either of three dimensional acceleration data. Which means vertical acceleration measurement cannot be taken directly through the accelerometer data.

According to rules of physics the only force the accelerometer gets in the stable condition is of gravity, which is downward, with a value equal to 1 g. This condition is fulfilled mathematically as in equation 4.

$$\overline{A_x} * \overline{A_x} + \overline{A_y} * \overline{A_y} + \overline{A_z} * \overline{A_z} = 1 \quad (4)$$

Where  $\overline{A_x}$ ,  $\overline{A_y}$  and  $\overline{A_z}$  are average acceleration values of x, y and z axes in stable section. Using these average acceleration values we can derive vertical acceleration projection as in equation 5.

$$\alpha_v = \frac{A \cdot \overline{A}}{|\overline{A}|} = A_x * \overline{A_x} + A_y * \overline{A_y} + A_z * \overline{A_z} \quad (5)$$

IRI quantifies smoothness of pavement surface based on the response of moving vehicle. It is expressed in meters per kilometre (m/km). Based on its definition, its formulation can be expressed as shown in equation 6.

$$IRI = \frac{\iint_{tstart}^{tstop} |\alpha_v|(dt)^2}{S} \quad (6)$$

Where  $IRI$  is International Roughness Index,  $tstart$  is starting time,  $tstop$  is the stopping time and  $S$  is the distance.

## 3 FINDING STABLE SECTION

The stable section refers to the duration of ride in which the cycle remains steady, for five seconds. Meaning the only force acting on the device in this duration is gravity. Identifying this stable section is crucial because the vertical acceleration component cannot be directly obtained from the accelerometer data due to the variable orientation of both the bicycle and the action camera. Thus, the authors (Zang, Shen, Huang, Wan and Shi, 2018) had to request the bicycle rider to keep the speed and posture as stable as possible for initial 5 seconds. Therefore, we propose finding this stable section autonomously.

We started with rolling variance and created an algorithm to find stable section. Rolling variances were calculated, over a window of 500 samples of the data from gyroscope using the equation 7.

$$RV = \frac{1}{N-1} \sum_{i=t-N+1}^t (x_i - \mu_t)^2 \quad (7)$$

Where  $RV$  is rolling variance,  $N$  is the size of the rolling window i.e the number of observations considered at each step,  $x_i$  is the value of the time series at time  $i$ .  $\mu_t$  is the rolling mean average at time  $t$  which is calculated using the equation 8.

$$\mu_t = \frac{1}{N} \sum_{i=t-N+1}^t x_i \quad (8)$$

Use of algorithm 1, provides variance details of the most stable section of the ride, excluding the part in which cyclist stops and rides with speed less than 11 km/h. From this stable section we calculate average acceleration values of x, y and z axes, which are used to calculate the vertical acceleration.

**Define Parameters:** Set the rolling window size  $W=500$  for variance calculations.

**Compute Rolling Variances:** For each gyroscope axis ( $-Y$  [rad/s],  $-X$  [rad/s], and  $Z$  [rad/s]), calculate the rolling variance over the window  $W$ .

Combine the computed variances and calculate the average variance for each window.

**Sort by Average Variance:** Sort the dataset based on the average variance in ascending order to prioritize the lowest variances.

Iterate and Identify the First Significant Variance: Initialize a flag `found_first = False`.

For  $i=1$  till `total_rows`:

    Compute the starting and ending indices of the rolling window.

    Calculate the cumulative sum of distances within this window.

    If the cumulative distance exceeds  $D$  threshold (cycle needs to be moving) and no significant variance has been found.

    Record the corresponding details: Rank, index range and average variance value.

    Set `found_first` to True and exit the loop.

**Output Results:** Return the first significant variance's details.

Algorithm 1: Finding stable section.

## 4 METHODOLOGY

The methodology describes a systematic process for assessing pavement surface. The flowchart of our methodology is shown in figure 1. Initially, pavement surface data is collected as the bicycle moves along the cycleway. Following, metadata is extracted from video file and unnecessary data (video and audio) is removed to abide by GDPR. The remaining data undergoes data cleaning and processing, including the removal of redundant values and interpolation for consistency. Later, the autonomous simplified quarter-car model for bicycles

is applied to analyze pavement roughness by processing sensor data.

In this study, GoPro Hero 9 action camera is used due to its compact design, integrated sensing capabilities and ease of deployment. It combines high-frequency inertial and positional data acquisition in a portable and cost-effective device.

The primary data for roughness assessment comes from the Bosch BMI260 IMU, operating at a sampling rate of 200 Hz. This IMU comprises a three-dimensional accelerometer, which measures linear accelerations, and a three-dimensional gyroscope, which captures angular velocities. Positional data is recorded via the UBlox UBX-M8030-CT GPS module, which works at a frequency of 10 Hz (Gopro, 2024). This allows precise geotagging of IMU data, mapping surface roughness to specific locations along the cycleway.

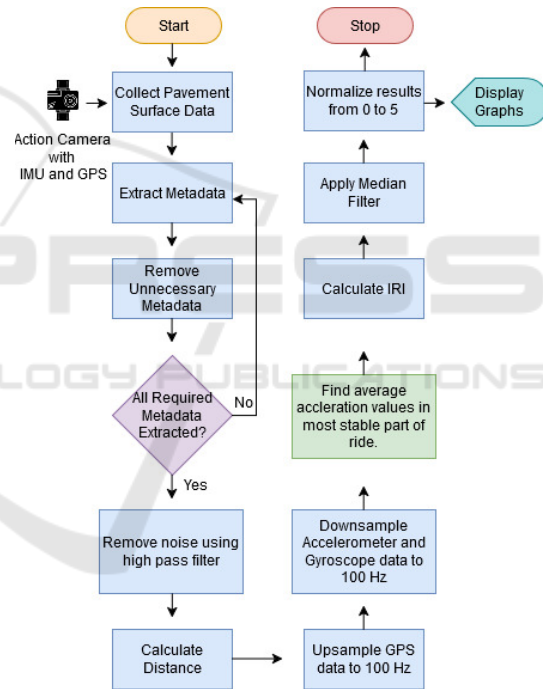


Figure 1: Shows flowchart of methodology.

The placement and orientation of the device have a direct impact on the quality of data collection. Misplaced sensors can result in misaligned data, thereby reducing pavement roughness accuracy. Mounting the device on the centre of the bicycle handlebar maintains a perfect symmetry between the stability and sensor data collection (Westerhuis and Waard, 2016). Thus, it is extremely important to mount it at optimal position, as shown in figure 2.

The action camera produces video file that contain embedded metadata. This metadata was

$$S = 2 * R * \arcsin \sqrt{\sin^2 \left( \frac{\varphi_2 - \varphi_1}{2} \right) + \cos(\varphi_1) * \cos(\varphi_2) * \sin^2 \left( \frac{\lambda_2 - \lambda_1}{2} \right)} \quad (9)$$

extracted using the GoPro Metadata Format parser available on GitLab (GoPro, 2024). Useful metadata includes timestamps, accelerometer, gyroscope and GPS data.

We used Haversine Formula (Sinnott, 1984) to compute distance using GPS locations. It calculates the distance between two geographic points, incorporating the curvature of the Earth. Its formula is shown in equation 9. Where  $S$  is distance,  $\varphi_1$  and  $\lambda_1$  are latitude and longitude of point 1,  $\varphi_2$  and  $\lambda_2$  are latitude and longitude of point 2, and  $R$  is the Earth radius (mean radius = 6371 km).

The cubic spline interpolation method was used to up-sample GPS location data from 10 Hz to 100 Hz. This method generates a smooth curve that passes through the original data points, ensuring a continuous and natural trajectory between recorded locations. By interpolating additional data points at higher frequency intervals, it helps maintain smoothness in the time-series data, which is essential for sensor fusion and further calculations.

The same cubic spline interpolation technique was also applied to down-sample accelerometer and gyroscope data from 200 Hz to 100 Hz. Instead of simple decimation (which removes excess samples), interpolation was used to construct a new 100 Hz signal by fitting a smooth curve through the original 200 Hz data points. This ensures that the reduced dataset maintains continuity and minimizes aliasing and loss of critical motion information.

By applying interpolation in both up-sampling and down-sampling, the time-series data remains smooth and well-aligned across different sensor modalities, improving the accuracy of sensor fusion and subsequent analysis.

Using the gyroscope data, equation 7, equation 8, and algorithm 1 we determine the most stable part of the ride from which we calculated average acceleration vector. After computing this vector, we used it in equation 5 to find the true vertical accelerations.

Previous computation provides all the necessary data to compute IRI. Thus, the IRI is calculated using equation 6. The calculation results were divided in 3 parts. Invalid, unable to calculate and the actual reading. Invalid section is the one in which either the cyclist stopped or moved at speed less than 11 km/h. The unable to calculate part is the one in which there was missing data reading from any of the sensors. The actual reading part was utilized for further analysis.

IRI is a common way to measure road roughness, but it has some limitations when used for cycleways. Cyclists naturally move while riding, which creates sudden fluctuations in IRI values that do not reflect actual pavement roughness. Moreover, different vehicles react differently to the same road surface, direct IRI values can sometimes give misleading results when analysing cycleway conditions.

For better analysis, we utilized CRI. First, a moving median filter is applied to smooth the IRI values. This filter slides over the data, replacing each value with the median over a 5-meter window. By reducing sharp fluctuations caused by human movement, it ensures that only meaningful roughness variations remain.

The second step is quantization ( $Q(IRI_s)$ ), where the smoothed IRI ( $IRI_s$ ) values are assigned to fixed levels based on specific intervals, as shown in equation 10. This process simplifies roughness variations, ensuring more consistent and comparable measurements. Quantization ensures that roughness measurements from different vehicles can be compared more effectively by eliminating minor differences caused by vehicle dynamics. Through these two steps, CRI provides a more stable and interpretable measure of cycleway pavement roughness. Additionally, setting a threshold of 8.5 helps filter out extreme variations that might not be relevant to actual surface roughness.

$$Q(IRI_s) = \begin{cases} 0, & 0 \leq IRI_s \leq 0.5 \\ 1, & 0.51 \leq IRI_s \leq 1.5 \\ 2, & 1.51 \leq IRI_s \leq 2.5 \\ 3, & 2.51 \leq IRI_s \leq 3.5 \\ 4, & 3.51 \leq IRI_s \leq 4.5 \\ 5, & 4.51 \leq IRI_s \leq 5.5 \\ 6, & 5.51 \leq IRI_s \leq 6.5 \\ 7, & 6.51 \leq IRI_s \leq 7.5 \\ 8, & 7.51 \leq IRI_s \leq 8.5 \end{cases} \quad (10)$$

## 5 EXPERIMENTS AND RESULT

Two experiments were performed to evaluate the effectiveness of the proposed model assessing cycleway pavement roughness. The first experiment analyses performance across diverse tracks, ensuring its capability to capture roughness under different conditions. The second experiment compare model consistency and reliability when applied to different

types of bikes, highlighting its adaptability to various vehicle configurations.

Bikes used for these experiments were manufactured from renowned companies. They were selected based on market availability and their suitability for use on paved roads. They were in their original condition, without any modifications.

Data was collected by adult volunteers who consented to process their personal data. Cyclists wore safety equipment and collected data in compliance with GDPR. The bikes were ridden on asphalt cycleways. Ethical approval for data collection was obtained beforehand.

### 5.1 Experiment 1

The 1<sup>st</sup> experiment was conducted to evaluate the performance of the proposed model across diverse cycle tracks. The assessment focused on data accuracy, reliability, and result consistency to comprehensively analyse the system’s overall effectiveness.

A volunteer, aged between 25 and 50 years, rode a manual bicycle across three cycle tracks in the northern region of Donegal, Ireland. A total of 11.66 kilometres of path data was processed. The specific track routes were as follows:

Track-1: From 54.906389° N, -8.309722° W to 54.930833° N, -8.318889° W.

Track-2: From 54.896111° N, -8.308611° W to 54.855278° N, -8.310556° W.

Track-3: From 54.834722° N, -8.332500° W to 54.855278° N, -8.310000° W.

This dataset provides a basis for analysing the model’s response to varying track conditions. Table 2 presents a summary of the key characteristics of each cycle track. Track 1, the shortest, spans 2,890.95 meters and features three intersections, two potholes and vegetation encroaching along the path. In contrast, Track-2, the longest at 5,374.33 meters, consists of eight intersections, 20 potholes, and significant vegetation coverage. Track 3, measuring 3,399.71 meters, lacks vegetation but includes five intersections and ten potholes, contributing to a varied cycling environment. The information was captured by manually looking the video after data capture from the GoPro camera. The selected tracks encompass a diverse mix of urban and rural terrains, incorporating steep gradients, smooth and uneven surfaces, potholes, sharp turns, intersections, and extended straight segments. These variations ensure that the evaluation considers a broad range of real-world cycling conditions.

Table 2: Show track statistics summary.

| Track | Number of Intersections | Number of Potholes | Presence of Vegetation | Distance (m) |
|-------|-------------------------|--------------------|------------------------|--------------|
| 1     | 3                       | 2                  | Yes                    | 2890.95      |
| 2     | 8                       | 20                 | Yes                    | 5374.33      |
| 3     | 5                       | 10                 | No                     | 3399.71      |

Bike used for this experiment was a manual bike, Trek 7100 Bike. Figure 2 shows this bike along with action camera. It is built with a lightweight aluminium frame having front suspension. It is equipped with 27.5 x 1.38-inch tires and powered by a 21-speed drivetrain, allowing it to adapt to various terrains with ease.



Figure 2: Trek 7100 Bike with action camera.

#### 5.1.1 Results of Experiment 1

The analysis focuses on the CRI values as a function of distance along each track, considering variations in track features such as length and track surface. All three tracks exhibited CRI values within the range of 0 to 5.

Figure 3 shows the results for track 1, where CRI values remain relatively stable at 1 for most of the track, indicating a smooth surface. The maximum CRI value recorded on this track was 5. The average CRI value for the entire track was 1.3. Minor spikes in the CRI values are observed indicating isolated sections of increased roughness. This increased roughness could be due to potholes and intersections. From these results, it is hard to conclude the actual effect of intersections, potholes and vegetation. However, it gives a holistic view of the ride roughness and quality.

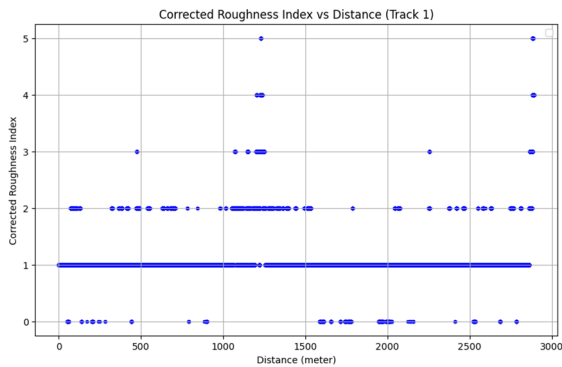


Figure 3: Track 1 results.

Track 2 exhibits similar fluctuations to those observed in track 1, as seen in figure 4, with CRI values mostly at 1, suggesting a smooth segment. Only one spot shows a CRI value of 5. Despite being the longest track, it recorded the lowest average CRI value of 1.2, which indicates a high-quality asphalt surface.

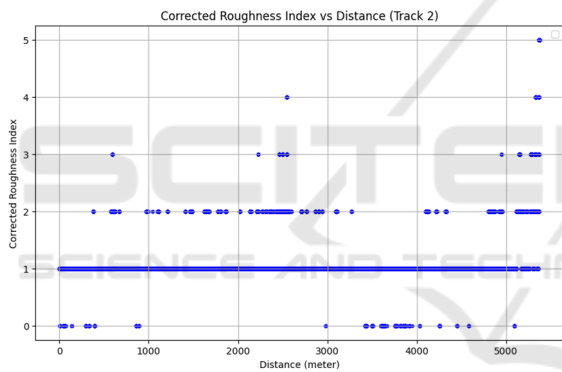


Figure 4: Track 2 results.

Figure 5 shows the results for track 3, which exhibits frequent variations in CRI values. The average CRI value for this track was 1.45. The smoother sections of track 3 indicate similar paving

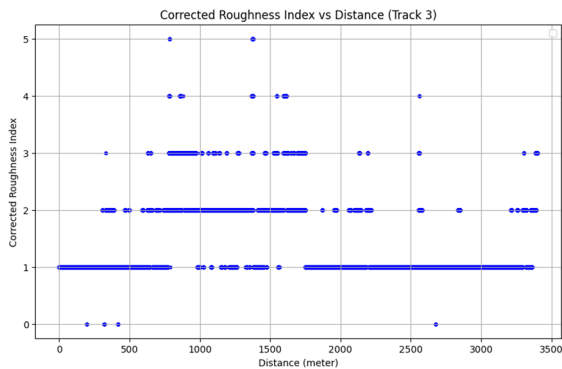


Figure 5: Track 3 results.

standards as of track 1 and track 2. Despite having fewer intersections and potholes than Track 2, the quality of Track 3 creates noticeable roughness at certain stretches along the track.

## 5.2 Experiment 2

The 2<sup>nd</sup> experiment was conducted to analyse the behaviour of the proposed model across different bicycles and evaluate its response to asphalt pavement characteristics. The study involved two cyclists, aged between 25 and 50 years, riding distinct bicycles on the same dedicated cycle track in Connemara, Ireland, under dry weather conditions. The total distance covered was 3.40 kilometres, starting from 53.45482° N, -9.86668° W and ending at 53.45681° N, -9.82077° W.

The experiment was conducted to compare the proposed model behaviour on different bikes. The assessment focuses on evaluating the asphalt pavement characteristics. The route represents a rural cycling environment with a combination of even and uneven terrain, vegetation coverage, straight stretches, six sharp turns, and two intersections.

The e-bike and e-scooter were equipped with a folding mechanism, pneumatic tires with different radius, disc brakes and a digital speedometer. Figure 6, include the Mirider One Folding Electric Bike (e-bike) and the Xiaomi Electric Scooter 4 Pro (e-scooter).



Figure 6: Mirider One Folding Electric Bike and Xiaomi Electric Scooter 4 Pro.

The Mirider One Folding Electric Bike features a magnesium alloy frame and a rear suspension system, designed for improved comfort on varying terrain. It is fitted with 16 × 1.75-inch pneumatic tires and powered by a 250W rear hub motor, enabling speeds of up to 25 km/h. The Xiaomi Electric Scooter 4 Pro is a lightweight aluminium alloy scooter equipped with 10-inch pneumatic tires. It is powered by a 350W front hub motor, capable of reaching a top speed of 25 km/h. These two distinct vehicle configurations provide a basis for comparing model performance, contributing to a more comprehensive understanding of road surface interactions.

## 5.2.1 Results of Experiment 2

The results were divided into 250-meter sections, to do comprehensive analysis of the cycleway roughness experienced by two cycles: e-bike and e-scooter. CRI values were calculated for both bicycles to evaluate the impact of road surface irregularities. Across all sections, e-bike exhibited higher CRI values, mostly clustering between 3 and 6, indicating a rougher ride. These values indicate that the e-bike was more sensitive to road surface irregularities.

On the other hand, e-scooter resulted with lower CRI values, clustering between 0 and 2, signifying a smoother ride. These lower values reflect the e-scooter's ability to handle surface unevenness more effectively, providing a smoother ride.

Varying degrees of bias in results is observed, as illustrated in figure 7, due to the tyre size and mechanical differences of bicycles. It compares CRI values for both cycles across section 1. In the plot, multiple distinct peaks are also visible at the same distances for both e-bike and e-scooter. Thus, indicating the reliability of the simplified quarter car model without requiring manual intervention, in identifying pavement surface conditions using bicycles.

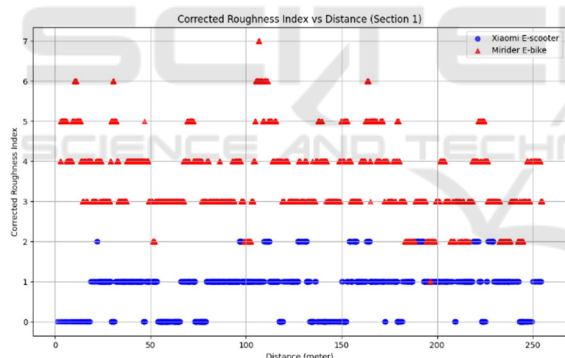


Figure 7: Section 1 results.

Furthermore, additional factors can introduce variability in roughness assessment. One potential source of error is the mounting position of the action camera, slight changes in placement alter vibration measurements. Environmental factors such as wind also play a crucial role in introducing bias in CRI measurements.

## 6 CONCLUSION AND LIMITATION

This research was conducted to evaluate the effectiveness of a simplified quarter car model for

cycles, without manual intervention, in assessing cycleway surface quality. The methodology utilizes proposed method to find stable section in order to calculate average acceleration vector.

For analysis, two experiments were carried out on paved asphalt cycleways. Cyclists rode action camera mounted bicycles and collected GPS and IMU sensor data. This data was processed using proposed model, and the results were further processed through CRI methodology.

In Experiment 1, the results showed that CRI values varied significantly with track features. The CRI values for all three tracks ranged from 0 to 5. Among three tracks, track 2 had the smoothest surface indicating a high-quality asphalt surface, while Track 3 exhibited the highest roughness and was assessed as having low quality asphalt surface. Track 1 had noticeable surface irregularities and was rated as having moderate asphalt quality surface.

In Experiment 2, the behaviour of the proposed model was assessed by riding different bicycles on the same track, focusing on evaluating asphalt pavement roughness. Two types of bicycles were used: an e-bike and an e-scooter. The results indicated bias such that the e-bike consistently experienced higher CRI values (between 3 and 6), and the e-scooter experienced lower CRI values (between 0 and 2).

Consistency in results indicate model's ability to identify rough patches. Its self-sufficiency nature points towards the method's tendency for scalability. Through which, on large scale, insights can be extracted to improve cycling infrastructure and enhance ride comfort.

While this study provides valuable insights into roughness measurements, certain limitations should be acknowledged. The experiments were conducted without considering camera data. This data would have helped to conclude deep insights about relation between track features and CRI.

Additionally, the absence of ground truth data for validation, limits the ability to directly assess the accuracy of the proposed model against established benchmarks. Another limitation is that the study was restricted to paved asphalt cycleways, excluding other surface types such as gravel paths, which could exhibit different roughness characteristics.

## 7 PRACTICAL IMPLEMENTATIONS

The proposed surface roughness assessment system is well-suited for real-world deployment due to its

reliance on commercially available action camera. The system can be integrated into smart city frameworks, allowing transportation departments to monitor cycleway conditions efficiently. By linking roughness data to county council infrastructure management systems, authorities can prioritize maintenance efforts, improving cycling safety and experience. Additionally, a web-based dashboard and mobile application could facilitate access to roughness metrics, enabling cyclists to make informed decisions about their routes. The autonomous nature of this system makes it scalable for city-wide deployment, reducing the need for manual intervention while ensuring continuous monitoring of cycling infrastructure.

## ACKNOWLEDGEMENTS

This research is conducted with the financial support of the EU commission Recovery and Resilience Facility under the Research Ireland OurTech Challenge Grant Number 22/NCF/OT/11220 and the support of Science Foundation Ireland under Grant number [SFI/12/RC/2289\ P2] the Insight SFI Research Centre for Data Analytics. The authors acknowledge support from Transport Infrastructure Ireland and Katleen Bell-Bonjean (Societal Impact Champion from GORTCYCLETRAILS.ie). For the purpose of Open Access, the author has applied a CC BY public copyright license to any Author Accepted Manuscript version arising from this submission.

## REFERENCES

- Alatoom, Y. I., & Obaidat, T. I. (2022). Measurement of street pavement roughness in urban areas using smartphone. *International Journal of Pavement Research and Technology*, 1-18.
- Fares, A., & Zayed, T. (2023). Industry-and academic-based trends in pavement roughness inspection technologies over the past five decades: A critical review. *Remote Sensing*, 15(11), 2941.
- GoPro. (2024, October 11). gpmf-parser [GitHub repository]. GitHub. <https://github.com/gopro/gpmf-parser>
- Hafizh, H., Abdullah, R., Ateeq, M., Majeed A., Isaac, M., Hu, B. (2023). Measurement and Analysis of International Roughness Index using IoT-based System. *IEEE Symposium on Wireless Technology & Applications*, 10249899.
- Hettiarachchi, C., Yuan, J., Amirkhanian, S., & Xiao, F. (2023). Measurement of pavement unevenness and evaluation through the IRI parameter—An overview. *Measurement*, 206, 112284.
- Sinnott, R. W. (1984). Virtues of the Haversine. *Sky and Telescope*, 68(2), 159.
- Kumar, L., Tallam, T., & Kumar, C. N. (2022, March). Assessment of ride quality and road roughness by measuring the response from a vehicle mounted Android smartphone. In *IOP Conference Series: Earth and Environmental Science* (Vol. 982, No. 1, p. 012062). IOP Publishing.
- Rizelioğlu, M., & Yazıcı, M. (2024). New approach to determining the roughness of bicycle roads. *Transportation research record*, 2678(1), 781-793.
- Sayers, M. W., Gillespie, T. D., & Queiroz, C. A. V. (1986). The international road roughness experiment: A basis for establishing a standard scale for road roughness measurements. *Transportation research record*, 1084, 76-85.
- Westerhuis, F., & De Waard, D. (2016). Using commercial GPS action cameras for gathering naturalistic cycling data. *Journal of the Society of Instrument and Control Engineers*, 55(5), 422-430.
- Woodstrom, J. H. (1990). Measurements, specifications, and achievement of smoothness for pavement construction (Vol. 167). *Transportation Research Board*.
- Yu, Q., Fang, Y., & Wix, R. (2022). Pavement roughness index estimation and anomaly detection using smartphones. *Automation in construction*, 141, 104409.
- Zang, K., Shen, J., Huang, H., Wan, M., & Shi, J. (2018). Assessing and mapping of road surface roughness based on GPS and accelerometer sensors on bicycle-mounted smartphones. *Sensors*, 18(3), 914.
- Zhang, Z., & Wenjiang, L. V. (2022, February). Research on theoretical evaluation method of road roughness based on smart-phone and whole vehicle model. In *Sixth International Conference on Electromechanical Control Technology and Transportation (ICECTT 2021)* (Vol. 12081, pp. 339-347). SPIE.